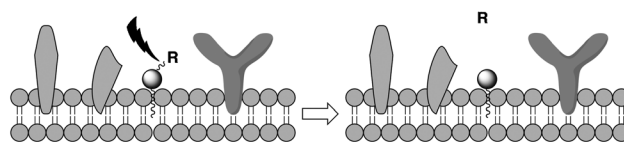


# Lipid Pools As Photolabile “Protecting Groups”: Design of Light-Activatable Bioagents\*\*

Luong T. Nguyen, Nathan P. Oien, Nancy L. Allbritton, and David S. Lawrence\*

Photolabile protecting groups<sup>[1]</sup> have found application in a wide assortment of arenas, including drug delivery, manipulation of intracellular biochemical processes (e.g. signaling pathways, gene expression), cell patterning for tissue fabrication, and both the production and application of nanoparticles, to name but a few. Genetically encoded light-activatable proteins provide an additional means (“optogenetic”) to manipulate biological systems with a high degree of temporal and spatial control.<sup>[2]</sup> However, whether based on optogenetic or optomolecular (non-gene-based) strategies, the design and construction of these species are derived from a series of well-defined principles. First, prior to photoactivation, the protected agent is biologically/biochemically/chemically inert. Second, light exposure generates a burst in active agent in a sufficiently rapid fashion to drive the desired process with the desired degree of spatiotemporal control. In the case of optomolecular systems, this is commonly achieved by covalently modifying a functional group (e.g. an alcohol) essential for activity with a photocleavable moiety (e.g. nitrobenzyl) that eliminates activity. However, there are many examples in which modification of only a single functional group is insufficient to block biological activity: oligonucleotides (e.g. antisense agents), peptides (e.g. protease substrates), and polymers in general (e.g. nanoparticles). We describe herein a design strategy that takes advantage of the compartmentalized nature of cells and organelles to create inert agents that can be activated upon a single photolytic event.

Biological membranes are composed of an inner lipophilic pool anchoring a protein layer that extends beyond the membrane surface. Nature commonly employs hydrophobic moieties (e.g. terpenes, cholesterol, peptides) to anchor proteins to membranes.<sup>[3]</sup> It occurred to us that lipidated bioactive species, retained by the membrane and hidden within the densely populated protein sheath, might be spatially incapable of acting on, or being acted upon by, their intracellular targets (Scheme 1). Insertion of a photolabile linker between the lipid (or other membrane-targeting



**Scheme 1.** General strategy for lipid pool-anchored light-activatable bioagents. The active species (R), when appended to a lipid, is embedded within the densely populated protein sheath and thus unavailable for interaction with its biological target. Photolysis releases R from the membrane and thus renders the bioagent active.

species) and the bioactive agent (“R” in Scheme 1) should furnish the means to release the bioactive species from the membrane in a light-dependent fashion.

The lipidated photolabile linker **1** (Scheme 2) contains a lipophilic C18 alkyl moiety and a carboxylate functionality to which bioactive active species can be appended. The benzylic C–N bond of the nitrobenzyl moiety is known to suffer photolysis at 360 nm,<sup>[1a]</sup> which should separate the bioagent from the lipophilic anchor and thus promote release of the now active species from the membrane surface.

For our initial studies, we prepared the lipidated 5-carboxytetramethylrhodamine (5-Tam)-side chain-modified lysine derivative **2**. LC–MS data confirmed that photolysis of **2** furnishes the corresponding lipid-free (5-Tam)-labeled lysine **3** (Supporting Information, Figure S3). The distribution and/or location of compound **2** and its photolyzed product **3** were assessed by fluorescence. Octanol/water partition studies revealed that 5-Tam fluorescence is exclusively observed in the octanol phase prior to photolysis (Figure 1 a, i) and primarily resides in the aqueous phase after photolysis (Figure 1 a, ii). In addition, compound **2** is retained by both mitochondria (Figure 1 b, i) and erythrocyte ghosts (Fig-

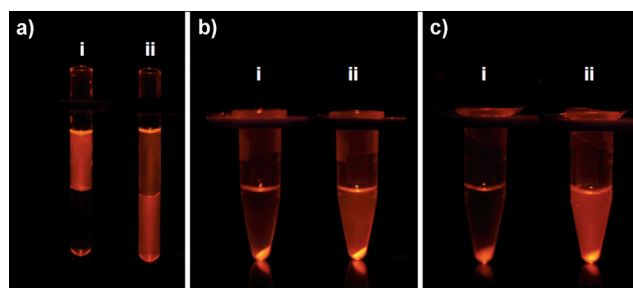
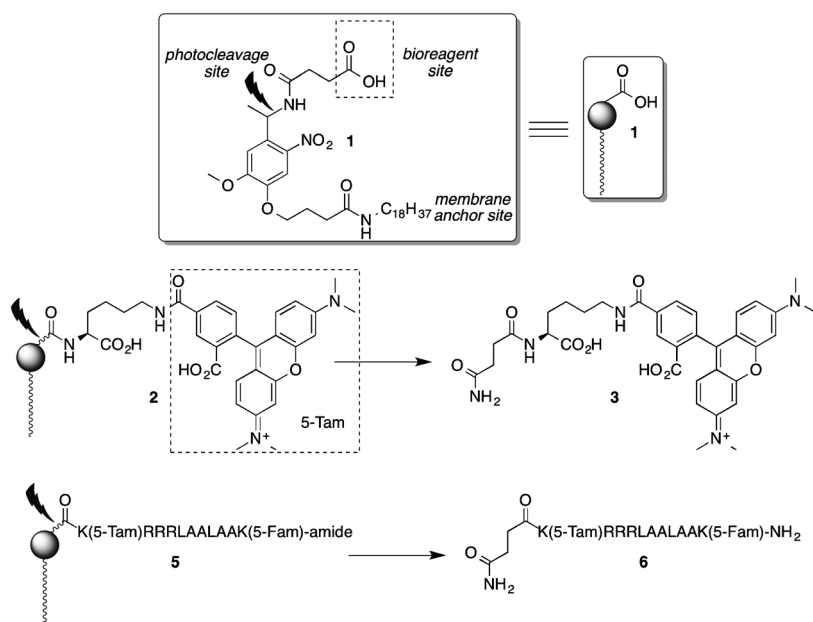


**Figure 1.** Light-dependent distribution studies with compound **2**. a) Distribution of **2** in octanol (top) and water (bottom) prior to (i) and after (ii) photolysis. b) Distribution of **2** in mitochondria (pellet) and buffer prior to (i) and after (ii) photolysis. c) Distribution of **2** in erythrocytes (pellet) and buffer prior to (i) and after (ii) photolysis.

[\*] L. T. Nguyen, N. P. Oien, Prof. N. L. Allbritton, Prof. D. S. Lawrence  
Department of Biomedical Engineering, Department of Chemistry,  
Division of Chemical Biology and Medicinal Chemistry, and the  
Department of Pharmacology  
University of North Carolina  
Chapel Hill, NC 27599 (USA)  
E-mail: lawrencd@email.unc.edu

[\*\*] We thank the NIH (CA140173) for financial support.

Supporting information for this article (including Materials and Methods, Tables, additional Figures, and Movies) is available on the WWW under <http://dx.doi.org/10.1002/ange.201305510>.



**Scheme 2.** Formulas of the photolabile lipitated linker **1**, a photolabile lipitated tetramethylrhodamine (5-Tam)-labeled lysine derivative **2** and its photolyzed product **3**, a photolabile lipitated protease sensor **5**, and the corresponding light-activated membrane-released derivative **6**.

ure 1 c, i). Subsequent release from the organelles/cells into the aqueous solution is triggered by light (Figure 1 b,c, ii).

We subsequently tested the hypothesis that bioactive species can be rendered biologically/biochemically inert by sequestration on membrane surfaces and then released/activated upon photolysis. We designed and synthesized the FRET-based peptide **4**, Ac-Lys(5-Tam)RRRLAALAAK(5-Fam)-amide (where 5-Fam = 5-carboxyfluorescein), which serves as a generic protease substrate. The corresponding lipitated derivative **5**, was prepared by replacing the N-terminal acetyl moiety in **4** with the photolabile linker **1**. The presence of the fluorophore 5-Fam, whose fluorescence is completely quenched by 5-Tam, furnishes the means to monitor substrate proteolysis at the 5-Fam emission wavelength (492 nm–525 nm). By contrast, the partially quenched 5-Tam signals the location of the peptide (555 nm–587 nm) both prior to and following photolysis (Figure S9). As indicated by fluorescence in an octanol/water partition study, **5** is directed to the octanol phase and photolysis releases the protease sensor into the aqueous phase. LC–MS data confirmed scission of the lipid anchor upon photolysis (Figure S4). Furthermore, when trypsin is present in the aqueous phase, only the photolyzed peptide (and not its unphotolyzed counterpart) suffers proteolysis (Figure S10). In the presence of mitochondria, **5** is likewise protected from trypsin-catalyzed proteolysis. Subsequent photolysis renders **5** sensitive to trypsinolysis, as indicated by the increase in fluorescence at 492 nm–525 nm (Figure 2; Figures S11–S13). Finally, in an analogous vein, absorption of **5** to erythrocyte ghosts renders the peptide nearly impervious to trypsinolysis, but photolysis leads to rapid proteolysis (Figure S14–S17).

We also examined the light-dependent behavior of the structurally distinct trypsin sensor **7**, in which the lipid anchor

is now cholesterol and sensitivity to hydrolysis is signaled by release of a coumarin<sup>[4]</sup> moiety (Scheme 3). As in the case of **5**, LC–MS was used to confirm the light-dependent release of the lipid anchor **8** from the sensor **7** (Figure S5). In analogy to **5**, erythrocyte-absorbed **7** is impervious to trypsinolysis, whereas the light-exposed erythrocyte-loaded **7** suffers release of active sensor (**9**) and subsequent rapid proteolysis in the presence of trypsin. The latter is readily observed in a real-time manner through the formation of the fluorescent product **10** (Figure S22).

In addition to proteolysis, we explored the susceptibility of a membrane-embedded protein kinase substrate to phosphorylation. The amino acid sequence, RRRLASLAA, is efficiently phosphorylated on the serine residue by the cAMP-dependent protein kinase (PKA) with ATP serving as the phosphoryl donor.<sup>[5]</sup> We prepared an analogue of this sequence, namely **11** which, like **5** and **7**, contains a lipid anchor appended to the photolabile nitrobenzyl moiety (Scheme 4). However, in this case, we employed a C12

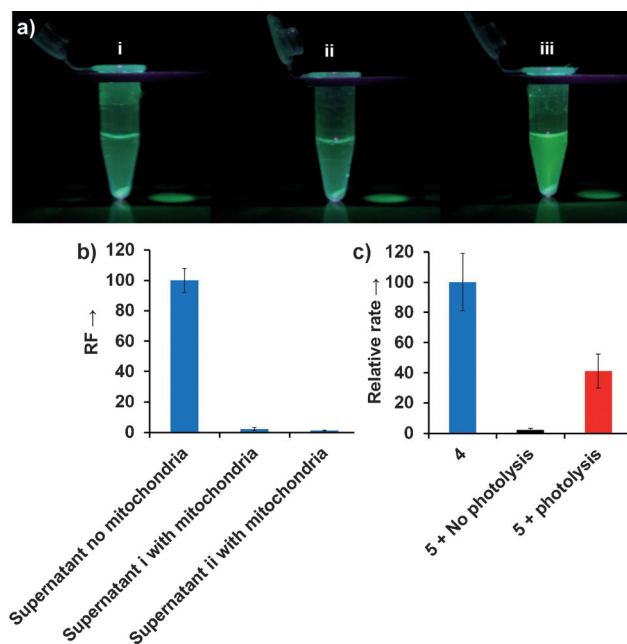
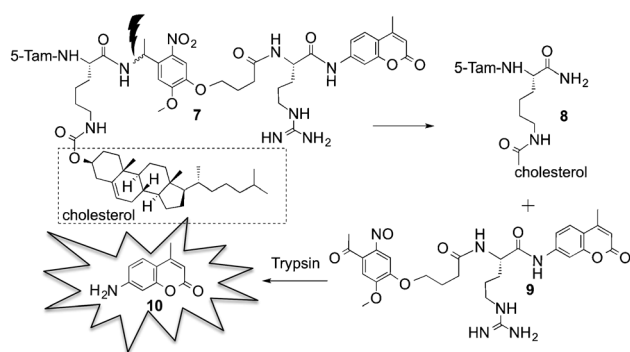
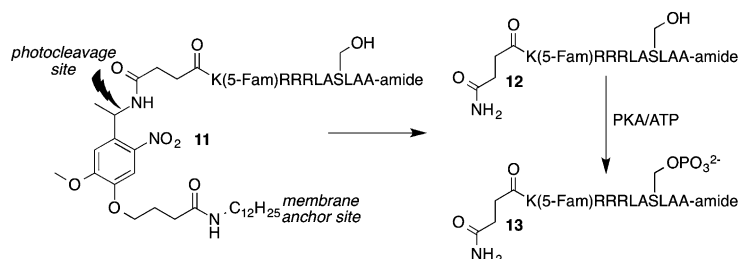


**Figure 2.** a) Trypsin cleavage of **5** loaded onto mitochondria in the absence and presence of illumination as assessed by fluorescence. Samples were illuminated with 360 nm UV light from a Hg-Arc lamp source, images were acquired with a 525 ± 25 nm band-pass filter. i) In the dark with trypsin; ii) with photolysis and no trypsin; and iii) with photolysis and trypsin after 40 min incubation at 37 °C. b) Relative amount of **5** in the supernatant in the absence and presence of mitochondria (supernatant i with mitochondria), and after a mitochondria wash (supernatant ii with mitochondria). c) Relative rate of trypsinolysis of **5** in the presence of mitochondria with and without photolysis compared to that of **4** (with mitochondria) as determined by fluorescence increase 492 nm–525 nm. RF = relative fluorescence.



**Scheme 3.** The inert trypsin sensor **7** is anchored using cholesterol to erythrocyte membranes. Photolysis releases the active sensor **9** that, upon trypsinolysis, furnishes a fluorescent response in the form of **10**.



**Scheme 4.** The inert PKA sensor **11** is anchored to biological membranes. Upon photolysis, the active sensor **12** is released and phosphorylated (**13**), as assessed by capillary electrophoresis.

lipid rather than the C18 analogue in **5**. We reasoned that, in spite of the reduced lipophilicity associated with C12, compound **11** might still predominantly associate with biological membranes owing to potentially favorable electrostatic interactions between the positively charged arginine residues on the peptide and the negatively charged lipid headgroups associated with the membrane. The lipidated-peptide **11** was incubated with mitochondria on ice for one hour and then centrifuged to collect the mitochondria in the pellet. The supernatant was collected and the pellet washed twice with buffer and the washings also collected. Based on these studies, more than 98 % of **11** is mitochondrially associated (Figure S23). Photolysis for two minutes at 360 nm releases approximately 50 % of mitochondria-embedded **11** (Figure S24). In addition, we compared the relative PKA-catalyzed phosphorylation rates (assessed by capillary electrophoresis) of **11**: 1) in the absence of mitochondria, 2) in the presence of mitochondria, and 3) in the presence of mitochondria followed by photolysis. As expected, when **11** is free in solution, it is efficiently phosphorylated by PKA. By contrast, mitochondria-bound **11** is inert to phosphorylation. The latter, upon photolysis, generates an active PKA sensor that undergoes PKA-dependent phosphorylation at a rate 50 % of that displayed by **11** that is free in solution. These results are consistent with the observed release of half of mitochondria-bound **11** during the two minute photolysis time period (Figure S25). In contrast to the protection offered by biological membranes, liposomes fail to render **11** resistant to phosphorylation (Figure S26). This observation is consis-

tent with that of Löwik and co-workers, who demonstrated that a mono-lipidated peptide is bioactive on a liposomal surface.<sup>[6]</sup> Based on these results, it is tempting to speculate that the cell's protein sheath, which is absent in liposomes, may protect cell-bound lipid-anchored species from biological processing until they are photolytically released. Interestingly, membrane-bound, peptide-based, FRET probes of macrophage MMP12<sup>[7]</sup> and neutrophil elastase<sup>[8]</sup> have been reported. However, in these instances, enzymatic activity resides on the cell surface.

Finally, we used one of the light-activatable sensors described above to assess endogenous intracellular biochemical activity. Erythrocytes are commonly thought of as little more than containers of haemoglobin.<sup>[9]</sup> However, there is a rich non-hemoglobin biochemistry associated with red blood cells, including biochemical pathways, such as glycolysis,<sup>[10]</sup> the presence of macromolecular catalytic complexes, such as the proteasome,<sup>[11]</sup> and as targets for various human diseases, such as malaria.<sup>[12]</sup> We assessed proteolytic activity of intact erythrocytes in a light-dependent fashion. The protease sensor **5** was loaded into the inner leaflet of erythrocytes using 2-hydroxypropyl- $\beta$ -cyclodextrin. Confocal images of **5**-embedded erythrocytes reveal that **5** is membrane-localized (Figure S18b). Photolysis was performed on a scanning confocal microscope using an integrated 355 nm continuous wave UV laser. The cleaved product of **5** is released into the erythrocyte interior (Figure 3; Figure S22b, Movie 1) as assessed by 5-Tam fluorescence. By contrast, there is no observable presence of the sensor in the interior of unphotolyzed

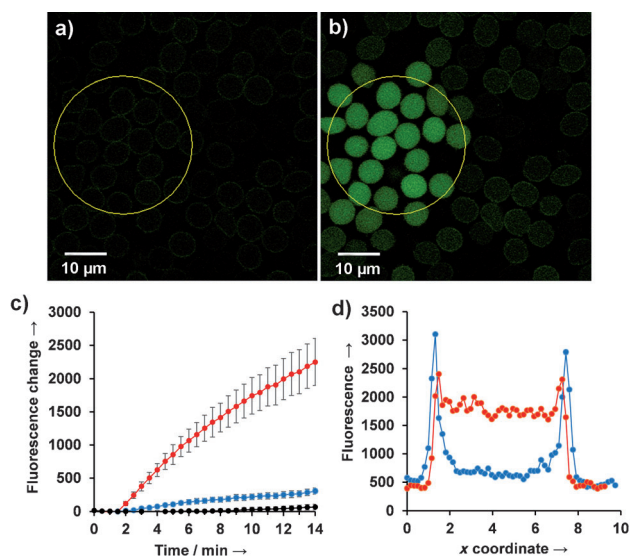


**Figure 3.** Confocal images of **5**-loaded erythrocytes before photolysis (a) and 13 min after photolysis (b). c) Average fluorescence inside photolyzed erythrocytes (red;  $n = 30$ ), unphotolyzed erythrocytes (blue;  $n = 30$ ), and photolyzed erythrocytes in the presence of a protease inhibitor cocktail (black; EDTA (10 mM), leupeptin (100  $\mu$ M), and MG-132 (100  $\mu$ M);  $n = 14$ ). d) Line scanning profile of a **5**-loaded erythrocyte before (blue) and 13 min after photolysis (red). Photolysis was performed with 100 mW, 355 nm laser at 1 mW, tornado mode, dwell time of 10  $\mu$ s pixel<sup>-1</sup>, and 5 frames.

erythrocytes. Furthermore, photoactivated cells display a robust increase in 5-Fam fluorescence, which serves as a barometer of proteolytic activity. Given the array of potential proteases that may act on **5**, we assessed the susceptibility of **5** to proteolytic degradation using erythrocyte lysates in the presence of various protease inhibitor combinations (Figure S20). The most potent combination (EDTA (10 mM), leupeptin (100  $\mu$ M), and MG-132 (100  $\mu$ M)) significantly inhibits sensor **5** proteolysis in erythrocyte lysates. In addition, this combination of protease inhibitors blocks the proteolytic degradation of photo-released **5** in intact erythrocytes as well (Figure 3c, Movie 2).

In summary, we have constructed lipidated light-responsive constructs that sequester bioagents to the membranes of organelles and cells. When membrane-bound, the bioagent is not susceptible to processing by its biological target. Photolysis releases the bioagent from its membrane anchor and thereby renders it biologically active. This strategy furnishes a means to control biological processes (be they intra- or intercellular) with a high degree of temporal resolution. In addition, the use of erythrocytes as carriers of photoactivatable agents provides intriguing possibilities in terms of drug delivery.<sup>[13]</sup>

Received: June 26, 2013  
Published online: July 31, 2013

**Keywords:** biosensors · cell adhesion · fluorescent probes · phosphorylation · photolysis

- [1] a) P. Klán, T. Solomek, C. G. Bochet, A. Blanc, R. Givens, M. Rubina, V. Popik, A. Kostikov, J. Wirz, *Chem. Rev.* **2013**, *113*, 119–191; b) H. M. Lee, D. R. Larson, D. S. Lawrence, *ACS Chem. Biol.* **2009**, *4*, 409–427; c) C. Brieke, F. Rohrbach, A. Gottschalk, G. Mayer, A. Heckel, *Angew. Chem.* **2012**, *124*, 8572–8604; *Angew. Chem. Int. Ed.* **2012**, *51*, 8446–8476.
- [2] G. Miesenböck, *Annu. Rev. Cell Dev. Biol.* **2011**, *27*, 731–758.
- [3] G. Charron, J. Wilson, H. C. Hang, *Curr. Opin. Chem. Biol.* **2009**, *13*, 382–391.
- [4] R. Lottenberg, U. Christensen, C. M. Jackson, P. L. Coleman, *Methods Enzymol.* **1981**, *80*, 341–361.
- [5] D. B. Glass, E. G. Krebs, *Annu. Rev. Pharm. Tox.* **1980**, *20*, 363–388.
- [6] M. B. Hansen, E. van Gaal, I. Minten, G. Storm, J. C. van Hest, D. W. Lowik, *J. Controlled Release* **2012**, *164*, 87–94.
- [7] A. Cobos-Correa, J. B. Trojanek, S. Diemer, M. A. Mall, C. Schultz, *Nat. Chem. Biol.* **2009**, *5*, 628–630.
- [8] S. Gehrig, M. A. Mall, C. Schultz, *Angew. Chem.* **2012**, *124*, 6363–6366; *Angew. Chem. Int. Ed.* **2012**, *51*, 6258–6261.
- [9] C. Z. Song, Q. W. Wang, C. C. Song, *Regul. Pept.* **2013**, *180*, 58–61.
- [10] R. van Wijk, W. W. van Solinge, *Blood* **2005**, *106*, 4034–4042.
- [11] S. Neelam, D. G. Kakhiashvili, S. Wilkens, S. D. Levene, S. R. Goodman, *Exp. Biol. Med.* **2011**, *236*, 580–591.
- [12] R. E. Farrow, J. Green, Z. Katsimitsoulia, W. R. Taylor, A. A. Holder, J. E. Molloy, *Seminars Cell. Develop. Biol.* **2011**, *22*, 953–960.
- [13] C. M. Hu, R. H. Fang, L. Zhang, *Adv. Healthcare Mater.* **2012**, *1*, 537–547.